ELSEVIER

Biochimica et Biophysica Acta 1285 (1996) 155–166

BIOCHIMICA ET BIOPHYSICA ACTA
BBA

# Evidence from incorporation experiments for an anionic channel of small conductance at the apical membrane of the rabbit distal tubule

N. Denicourt [a], S. Cai [a], L. Garneau [a], M.G. Brunette [b], R. Sauvé [a,*]

[a] *Department of Physiology, Membrane Transport Research Group, University of Montreal, C.P. 6128, Succ. Centre-ville, Montreal, Quebec H3C 3J7, Canada*

[b] *Maisonneuve Hospital, Montreal, Quebec, Canada*

Received 23 April 1996; revised 16 July 1996; accepted 17 July 1996

**Abstract**

Many of the hormone-regulated ion transport processes in distal nephron involve transcellular pathways which require a passive entry of ions at the apical membrane of the distal tubule cells. To investigate molecular mechanisms underlying the ionic permeability of the distal tubule apical membrane, a study was undertaken in which vesicles prepared from apical membranes from isolated rabbit distal tubules were fused onto a planar lipid bilayer. These experiments led to the identification of several ionic channels including a $Cl^-$-permeable channel of 14 pS with a $Na^+$ over $Cl^-$ permeability ratio, $P_{Na}/P_{Cl} < 0.09$. The open channel probability ($P_o$) showed a weak voltage dependency with $P_o$ increasing slightly at negative potential values (intracellular (trans) relative to extracellular (cis) for right-side-out vesicles). Channel activity was inhibited by NPPB at high concentrations (> 100 $\mu$M) and by DIDS (300 $\mu$M). A small inhibitory effect was also observed in the presence of DPC at concentrations ranging from 200 $\mu$M to 500 $\mu$M. The presence of $SO_4^{2-}$ (32 mmol/l) in the trans solution caused a complete inhibition of channel activity, but no modification of channel behaviour was observed with the non-selective channel blocking agent gadolinium ($Gd^{3+}$) at 100 $\mu$M. Finally, addition of the catalytic subunit of protein kinase A into the trans chamber (60 U/ml to 80 U/ml) led to an increase in channel activity characterized by a greater number of active channels coupled to an increase of the individual channel open probability. The action of the protein kinase A could be cancelled by the addition of a non specific protein phosphatase, such as alkaline phosphatase. Our results suggest that the apical membrane of the rabbit distal tubule contains a $Cl^-$ permeable channel of small conductance the activity of which may be modulated by hormones linked to the adenylate cyclase pathway.

*Keywords:* Distal tubule; Chloride channel; cyclic AMP; PTH

Abbreviations: CFTR, cystic fibrosis transmembrane conductance regulator; DIDS, 4,4'-diisothiocyanatostilbene-2,2'-disulfonic acid; DMSO, dimethyl sulfoxide; DPC, diphenylamine-2-carboxylic acid; Hepes, *N*-2-hydroxyethylpiperazine-*N'*-2-ethanesulfonic acid; NMDG, *N*-methyl-D-glucamine; NPPB, 5-nitro-2-(3-phenylpropylamine)benzoic acid; POPC, 1-palmitoyl-2-oleoylphosphatidylcholine; POPE, 1-palmitoyl-2-oleoylphosphatidylethanolamine; PTH, parathyroid hormone; Tris, tris(hydroxymethyl)aminomethane.

* Corresponding author. Fax: +1 (514) 3437146.


*PII* S0005-2736(96)00151-4

## 1. Introduction

The distal tubule plays a key role in the hormonal regulation of several essential ion transport processes in the kidney, including $Cl^-$ transport. It is now generally agreed that the control by hormones of the membrane $Cl^-$ permeability of distal tubule cells is linked in most cases to an increase in cAMP production [1]. For instance, two $Cl^-$ channels of small conductance (3 pS and 8 pS), one of which (3 pS) characterized by a cAMP-sensitive open probability, were identified at the apical membrane of A6 cells, a model cell line with distal tubule-like properties [2,3]. A cAMP-dependent $Cl^-$ channel of 9 pS was also reported in a recent patch clamp study by Poncet et al. [4] at the apical membrane of rabbit distal tubule cells in culture. This channel had many features in common with the CFTR channel family and resembled the $Cl^-$-selective channel of small conductance (9 pS) identified by Ling et al. [5] in the apical membrane of rabbit cortical collecting duct cells (CCT) grown in primary culture. The presence of cAMP activated $Cl^-$ channels was also confirmed at the basolateral membrane of distal nephron. For instance, cAMP-dependent $Cl^-$ channels were found in the mouse thick ascending limb of the loop of Henle and in RCCT-28A cells, an immortalized cell line derived from rabbit cortical collecting duct cells [6,7]. The functional role of these channels remains still to be fully established, but the $Cl^-$ channel at the basolateral membrane of the thick ascending limb is likely to be involved in $Cl^-$ ion reabsorption.

The role of hormone regulated $Cl^-$ channels in the distal nephron may not be limited to $Cl^-$ ion transport only. For example, results obtained from immortalized mouse distal convoluted cells have led to the proposal that the PTH-dependent $Ca^{2+}$ reabsorption in the distal nephron is stimulated following the activation of a NPPB-inhibitable $Cl^-$ conductance at the basolateral membrane [8]. According to this model, PTH would increase $Cl^-$ conductance in distal convoluted tubule cells, leading to decreased intracellular $Cl^-$ activity, membrane hyperpolarization and increased $Ca^{2+}$ entry [8,9]. The validity of this model and the exact nature of the proposed $Cl^-$ permeable channel need still to be confirmed, but the observed effect of NPPB on $Ca^{2+}$ uptake provides clear indication that the activation of $Cl^-$ channels by hormones may constitute an important mechanism for the regulation, via changes in membrane potential, of a large variety of voltage-dependent ion transport processes [8,9].

Although numerous studies have been reported concerning ion transport pathways in the distal tubule, direct evidence for apical $Cl^-$ channels in this segment is limited [1,4,10–14]. Moreover, most single channel studies performed so far have used cell lines (A6) or distal tubule cells in culture. To investigate the nature of the $Cl^-$ permeable channels at the apical membrane of the rabbit distal tubule, a study was undertaken in which vesicles prepared from native apical membranes of rabbit distal tubules were fused onto a planar lipid bilayer. This approach was chosen to avoid the potential problems due to the more or less severe cell dedifferentiation which takes place during cell culturing. The results of our study essentially indicate the presence at the apical membrane of distal tubule cells of a PKA-sensitive $Cl^-$ permeable channel of small conductance (14 pS), with biophysical and pharmacological properties different from those normally associated to the CFTR channel family.

## 2. Materials and methods

### 2.1. Vesicle preparation

Distal tubules were obtained from rabbit kidneys. It has to be mentioned that the term distal tubule in the present case refers to the distal convoluted tubule, the connecting tubule and the initial portion of the cortical collecting duct. The technique of tubule preparation has been described in details elsewhere [15,16]. Briefly, tubules were digested with collagenase and centrifuged on a Percoll gradient. The suspensions of distal tubules were mechanically homogenized (Dounce homogenizer), stirred for 10 min on ice after addition of 12 mmol/l $MgCl_2$ and finally centrifuged at $400 \times g$ for 20 min. The supernatant was collected and centrifuged at $45\,000 \times g$ for 20 min at 4°C. The new sediment, enriched in luminal membranes, was washed twice and suspended in 300 mmol/l mannitol, 15 mmol/l Hepes-Tris at pH 7.4. The resulting membrane preparations lacked alkaline phosphatase and Na-K-ATPase activity, but possessed a $Na^+$ transport sensitive to thiazides [15,16].

### 2.2. Single channel recording

#### 2.2.1. Planar bilayer formation

Planar lipid bilayers were formed at room temperature from a 1:1 mixture of POPC and POPE (Avanti Polar) dispersed in decane at a concentration of 20 mg/ml. The lipid bilayers were painted over a 200 $\mu$m hole drilled in a Delrin partition separating two solution-filled chambers of 3 ml (trans) and 5 ml (cis), respectively. The outline of the aperture was pretreated with a small amount of triglyceride prior to the application of the lipid suspension. Fusion of the vesicles was initiated mechanically by gently touching the bilayer from the cis side using a small stainless steel wire (Kerr) of 150 $\mu$m diameter, on the tip of which was deposited a small drop of the vesicles containing solution. For right-side-out vesicles, the cis chamber should correspond under these conditions to the extracellular medium.

#### 2.2.2. Data acquisition and analysis

Single channel currents were measured using either an Axopatch 200A or a List EPC7 amplifier. The trans chamber was voltage-clamped relative to the cis chamber which was grounded. Electrical connections were made by using Ag/AgCl electrodes and agar salt bridges (3 M KCl) to minimize liquid junction potentials. Signals were stored on videotapes (SONY, SL-300) and subsequently transferred on the hard disk of a PC computer. Recordings were digitized at sampling rates between 500 Hz and 3 kHz which corresponded to five times the cutoff frequencies chosen for filtering (8-pole Bessel: Frequency Devices 902). The unitary current amplitude and channel open probability were estimated from current amplitude histograms or from noise-free Markov signals generated by processing experimental current records using an algorithm based to the Baum–Welch re-estimation formulae [17]. For multi-channel recordings, the open probability was calculated assuming that the current levels were distributed according to a binomial statistics. The validity of the binomial distribution was tested by performing a $\chi^2$ analysis based on the procedure described previously [18]. For an ensemble of $N$ identical channels ($N \leq 5$), characterized by an open probability $P_o$, estimations of $N$ and $P_o$ could also be obtained through the Baum–Welch re-estimation formulae, by measuring the number of transitions/s between two adjacent current levels. For instance, with $N$ identical independent channels, $T_{r\rightarrow r+1}$, the number of transitions from the $r$ current level ($r$ channels open) to the $r+1$ current level ($r+1$ channels open) corresponds to $(N-r)K_1$ where $K_1$ is the average rate of transitions/s for a single channel from the ensemble of the non-conducting states to the ensemble of the conducting states. Similarly, $T_{r+1\rightarrow r+2}$, the number of transitions/s from level $r+1$ to level $r+2$ ($r+2$ channels open) is given by $(N-1-r)K_1$. An estimation of $N$ can readily be obtained from the ratio

$$\frac{T_{r\rightarrow r+1}}{T_{r+1\rightarrow r+2}} = \frac{(N-r)}{(N-1-r)} \tag{1}$$

This procedure was tested on stationary computer generated data and was found to yield accurate estimations of $N$ and $P_o$ as long as the distribution of the current levels obeyed a binomial distribution. This approach was especially useful in cases where current amplitude histograms failed to show the $N+1$ distinct current levels.

The stationarity of single channel recordings was tested using a method adapted from Kendall and Stuart [19]. Essentially, a sequence was created of $M$ uncorrelated mean current values $\{\langle I\rangle_1, \langle I\rangle_2, \langle I\rangle_3,..\langle I\rangle_i,..\langle I\rangle_j,..\langle I\rangle_M\}$ obtained by averaging single channel currents over $M$ equal successive time periods. The duration of the time period was typically of 1 s. We then defined a stochastic variable A such that:

$$A = \sum_{i}^{} \sum_{<j} a_{ij} \tag{2}$$

where for $1 \leq i \leq M-1$ and $i < j \leq M$

$$a_{ij} = \begin{cases} 1 & \text{if } \langle I\rangle_j > \langle I\rangle_i \\ 0 & \text{otherwise} \end{cases} \tag{3}$$

It can be shown that the average value of $A$ in a random sequence of integers is

$$\langle A\rangle = \frac{M(M-1)}{4} \tag{4}$$

and that the variance of A corresponds to

$$\sigma_A^2 = \frac{2M^3 + 3M^2 - 5M}{72} \tag{5}$$

For $M > 10$, the distribution of $A$ may be closely approximated by a normal distribution. Stationarity

was accepted as long as $A$ falls within a 95% confidence interval.

Channel ionic selectivity was computed from the constant field equation using

$$\Phi^2\left[-P_{Na}[Na]_o - P_{Cl}[Cl]_i - 4P_{Ca}[Ca]_o\right] + \Phi\left[P_{Na}([Na]_i - [Na]_o) - P_{Cl}([Cl]_i - [Cl]_o)\right] + \left[P_{Na}[Na]_i + P_{Cl}[Cl]_o + 4P_{Ca}[Ca]_i\right] = 0 \quad (6)$$

with

$$\Phi = e^{-\frac{Vq}{kT}} \quad (7)$$

where $V$ is the applied potential (trans relative to cis), $q$ the electronic charge, $k$ Boltzmann's constant and $T$ the temperature. Single channel current–voltage ($I$–$V$) curves were determined for a given set of ionic conditions, and the experimental value for the reversal potential obtained by means of a linear interpolation procedure. The resulting value was compared to the equilibrium potential for $Cl^-$ ions prevailing under these ionic conditions. For monovalent ions, $\delta V$, the difference between the measured reversal potential and $E_{Cl}$, the equilibrium potential expected for a $Cl^-$-selective channel, corresponds to

$$\delta V = 25 \ln \left[ \frac{1 + \alpha \frac{[X^+]_{cis}}{[Cl^-]_{trans}}}{1 + \alpha \frac{[X^+]_{trans}}{[Cl^-]_{cis}}} \right] \quad (8)$$

where $\alpha$ is the permeability ratio $P_X/P_{Cl}$. Because of the uncertainty concerning the $Cl^-$ ion activity in salt solutions containing divalent cations such as $Ca^{2+}$, the expected equilibrium potentials for $Cl^-$ ions, including the contribution of the junction potentials coming from the salt bridges, were estimated by measuring the difference in potential generated between two Ag/AgCl electrodes placed in 1 ml chambers that contained, respectively, the cis and trans solutions used for the bilayer experiments. The chambers were electrically connected via a 3 M KCl agar bridge, and the electrodes were allowed to equilibrate overnight. The reversal potential values, $E_{Cl}$, expected for a $Cl^-$-selective system in various ionic conditions are presented in Table 1.

Table 1
Experimental estimation of the $Cl^-$ ion equilibrium potential for the various salt solutions used for channel incorporation experiments

| Trans solution (mmol/l) | Cis solution (mmol/l) | $E_{Cl}$ (mV) |
|---|---|---|
| 50 $CaCl_2$ | 200 $CaCl_2$ | $-24.9 \pm 0.8$ ($n = 3$) |
| 50 $CaCl_2$ | 200 NaCl + 1 $CaCl_2$ | $-12.5 \pm 0.8$ ($n = 3$) |
| 50 NaCl | 200 NaCl + 10 $CaCl_2$ | $-30.0 \pm 1$ ($n = 3$) |

### 2.3. Materials

Salts, reagents and solvent were analytical grade. NPPB and DPC were purchased from RBI (Research Biochemicals, Natick, MA) and DIDS from Sigma (St. Louis, MO). Stock solutions were prepared in DMSO. DMSO (1%) alone was without effect on channel activity. NMDG solutions were prepared by titrating with HCl. The catalytic subunit of the protein kinase A was obtained either from Sigma (bovine heart; #P-2645) or from Boehringer Mannheim (bovine heart; #1 529 307). Alkaline phosphatase was purchased from Boehringer Mannheim (calf intestine; #1 097 075). The pH of the solutions was adjusted to 7.3 with Tris-Hepes.

## 3. Results

### 3.1. Channel conductance and selectivity

Channel incorporation experiments carried out with vesicles prepared from apical membranes of rabbit distal tubules led to the identification of at least three different types of anion permeable channels. Fig. 1 illustrates the single channel events most frequently observed in 200 mmol/l (cis)/50 mmol/l (trans) $CaCl_2$ conditions. These experimental conditions were chosen as to improve vesicle fusion while minimizing the potential contribution of $K^+$ and/or $Na^+$ channels. High $Ca^{2+}$ solutions enabled furthermore the detection of low conductance $Ca^{2+}$-selective channels such as the one reported in mouse distal convoluted tubule cells [8,9]. Our incorporation experiments failed, however, to reveal the presence of $Ca^{2+}$ channels in vesicles prepared from apical membranes of isolated rabbit distal tubules. The results in Fig. 1 show clear upward current jumps at potentials

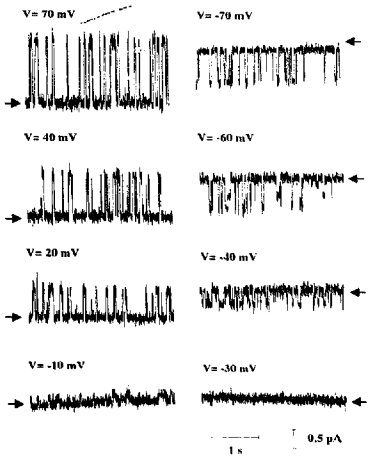


Fig. 1. Examples of single channel recordings in 200 mmol/l (cis)/50 mmol/l (trans) $CaCl_2$ conditions measured at transmembrane potentials (trans relative to cis) ranging from −70 mV to 70 mV. Subconductance levels are apparent at −60 mV. Arrows indicate the channel closed state current levels. The signal was filtered at 100 Hz and sampled at 500 Hz.

positive to −10 mV, while downward current transitions became detectable at potentials more negative than −40 mV. This suggests a reversal potential value within the voltage range −20 mV to −30 mV. Channel activity occurred in a large number of recordings as current bursts separated by silent periods of a few seconds to hundred of seconds duration (Fig. 2A). Recordings characterized by long closures were not usually considered for open probability ($P_o$) measurements, the evaluation of $P_o$ being too uncertain when taken from current records that were limited for practical reasons to 1 or 2 min. There were, however, no apparent changes in the burst and interburst duration as a function of the applied voltage. This particular channel was also characterized by current transitions involving a sub-conducting state (Fig. 1 at $V = -60$ mV and Fig. 2B). The presence

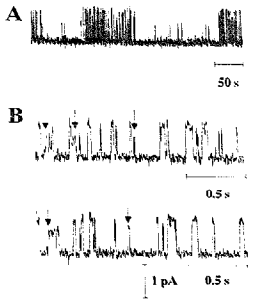


Fig. 2. (A) Example of the channel bursting activity. Recording performed in 200 mmol/l (cis)/50 mmol/l (trans) $CaCl_2$ conditions at an applied voltage of 40 mV. (B) Examples of transitions to an intermediate conductance level. Arrows indicate transitions to a level corresponding to 60% of the full conducting state. Experimental conditions as in (A). Record sampled at 500 kHz and filtered at 150 Hz.

of an intermediate conductance level was confirmed in most of our experiments, but its effect on current amplitude histograms appeared negligible due to its low probability of occurrence. The channel current–voltage relationship for the full conducting state is presented in Fig. 3. Data were obtained from 10 independent experiments performed in 200 mmol/l (cis)/50 mmol/l (trans) $CaCl_2$ conditions. The cur-

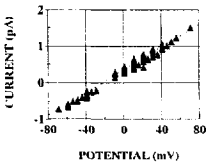


Fig. 3. Global single channel $I-V$ curve measured in 200 mmol/l (cis)/50 mmol/l (trans) $CaCl_2$ conditions. Results obtained from 10 different experiments. The reversal potential estimated by linear regression was $-24 \pm 3$ mV for a permeability ratio $P_{Cl}/P_{Ca} \gg 1$ (see Eq. (8) in Section 2). The resulting $I-V$ curve had a near ohmic behaviour with a slope conductance of $14 \pm 2$ pS.

rent–voltage relationship showed an outward rectification over the voltage range considered, with a slope conductance for positive currents of $14 \pm 2$ pS ($n = 10$). The reversal potential was estimated by linear regression at $-24 \pm 3$ mV ($n = 10$), a value in agreement with the expected reversal potential for a $Cl^-$-permeable system with $P_{Cl}/P_{Ca} \gg 1$ (see Table 1). Finally, channels of higher conductances were also observed in several recordings, but their low probabilities of occurrence prevented any detailed single channel characterization.

The channel ionic selectivity was next investigated in experiments in which the cis and trans chambers contained 200 mmol/l NaCl + 1 mmol/l $CaCl_2$ and 50 mmol/l $CaCl_2$, respectively. Most of these experiments failed to show single channel activity in the absence of $Ca^{2+}$ at concentrations ranging from 1 mmol/l to 10 mmol/l in the cis compartment. This observation was interpreted as indicating that $Ca^{2+}$ may be essential to the fusion process despite the close contact between the vesicles and the membrane which was initiated mechanically in our case. Current jumps associated to a 14 pS $Cl^-$ channel could be observed, however, in 200 mmol/l $CaCl_2$ (cis)/50 mmol/l MNDG-Cl (trans) conditions, indicating that channel incorporation was independent of the $Ca^{2+}$ concentration in the trans compartment (see Fig. 10A). Fig. 4 presents typical single channel records obtained under 200 mmol/l NaCl + 1 mmol/l $CaCl_2$ and 50 mmol/l $CaCl_2$ conditions. The resulting $I$–$V$ curve computed from four different experiments is presented in Fig. 5A. The $I$–$V$ relationship showed a weak rectification within the voltage range −60 mV to 60 mV, with a slope conductance at positive currents of 11 pS. The reversal potential was estimated by linear regression at $-6.5 \pm 3$ mV, for a value of $\delta V$, the potential difference relative to the $Cl^-$ equilibrium potential measured under identical ionic conditions, of 6.0 mV (see Section 2). On the

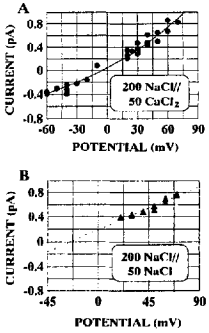


Fig. 5. (A) Global single channel $I$–$V$ curve in 200 mmol/l NaCl + 1 mmol/l $CaCl_2$ (cis)/50 mmol/l $CaCl_2$ (trans) conditions. Results from three different experiments. The reversal potential was estimated by linear regression at $-6.5 \pm 3$ mV for a permeability ratio $P_{Na}/P_{Cl} < 0.12$. The resulting $I$–$V$ curve showed a weak rectification within this voltage range (−60 mV to 60 mV) with a slope conductance at positive currents of 11 pS. (B) Single channel $I$–$V$ curve in 200 mmol/l NaCl + 10 mmol/l $CaCl_2$ (cis)/50 mmol/l NaCl (trans) conditions. The slope conductance was equal to 10 pS with a mean reversal potential value of −22 mV ($n = 3$), for an effective $P_{Na}/P_{Cl}$ ratio < 0.09.

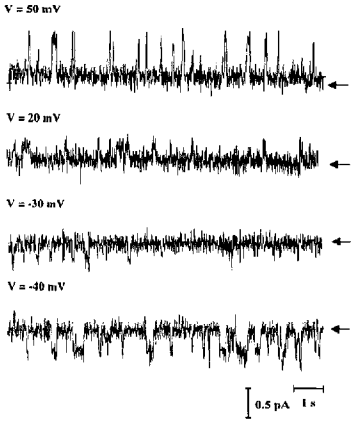


Fig. 4. Examples of single channel recordings measured in 200 mmol/l NaCl + 1 mmol/l $CaCl_2$ (cis)/50 mmol/l $CaCl_2$ (trans) conditions for transmembrane potentials ranging from −40 mV to 50 mV. Arrows indicate the channel closed state current levels. The signal was filtered at 100 Hz and sampled at 500 Hz.

basis of Eq. (8), these observations yield a $Na^+$ over $Cl^-$ permeability ratio, $P_{Na}/P_{Cl} < 0.12$ ($P_{Ca}/P_{Cl}$ was set equal to zero). This value was confirmed in experiments carried out in 200 mmol/l NaCl + 10 mmol/l $CaCl_2$ (cis)/50 mmol/l NaCl (trans) conditions (Fig. 5B). The mean zero current potential value corresponded to $-22 \pm 3$ mV in this case ($n = 3$), for a mean $\delta V$ of 8 mV and an effective $P_{Na}/P_{Cl} <$ 0.09 (see Eq. (8)). However, due to the small amplitude of the current jumps at potentials negative to $-20$ mV, unambiguous current values could not be obtained within that voltage range. This is at variance with the results presented in Fig. 5A and may be partly related to a lower trans $Cl^-$ concentration in 50 mM NaCl compared to 50 mM $CaCl_2$ conditions. These experiments provided nevertheless evidence that the 14 pS anionic channel present in this vesicle preparation is mainly permeable to $Cl^-$ ions.

### 3.2. Voltage dependence of the channel open probability

The integrity of the 14 pS channels obtained by incorporation was assayed by means of a binomial analysis of the recordings which contained multiple channels. This approach was used to test the hypothesis that the multi-channel activity observed in these cases corresponded to the superposition of identical 14 pS channels. Such analysis is essential to confirm that the 14 pS channels we observed still constitute after channel incorporation an homogeneous channel population. The upper panels in Fig. 6 present current traces with multiple channels while the lower panels show the resulting binomial analysis. The current records were measured in 200 mmol/l (cis)/50 mmol/l (trans) $CaCl_2$ conditions. The idealized signals were obtained by applying the Baum–Welch re-estimation algorithm to each of the experimental current traces shown (see Section 2). The current level distribution measured at both voltages was found to follow a binomial statistics with three independent channels characterized by open probability of 0.18 and 0.34 at 30 mV and $-60$ mV, respectively. The presence of three independent channels was further confirmed by measuring the ratio $T_{0\to1}/T_{1\to2}$ as described in Section 2. The overall results of this analysis are presented in Table 2. Estimation of the ratio $T_{0\to1}/T_{1\to2}$ in both cases led to values close to 3/2, the predicted ratio $T_{0\to1}/T_{1\to2}$ for a system consisting of three independent channels. This agree-

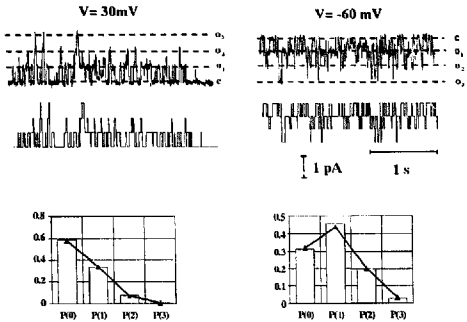


Fig. 6. Binomial analysis of multiple channel recordings. Current records measured in 200 mmol/l (cis)/50 mmol/l (trans) $CaCl_2$ conditions. The idealized signals result from the application of a Baum–Welch re-estimation algorithm to the corresponding experimental current traces. C refers to the current level with no channel open, while $o_n$ corresponds to the current level when $n$ channels are open. $P_{(n)}$ refers to the probability of having $n$ channels open at the same time. The current level distribution was found to obey a binomial statistics, with three channels characterized by an open probability, $P_o$, of 0.18 at 30 mV and $P_o = 0.34$ at $-60$ mV.

Table 2
Multi-channel analysis based on the Baum–Welch re-estimation formulae

| V(mV) | $T_{0\to1}$ (1/s) | $T_{1\to2}$ (1/s) | $T_{1\to0}$ (1/s) | $T_{2\to1}$ (1/s) |
|---|---|---|---|---|
| 30 | 25 | 17 | 43 | 81 |
| −60 | 43 | 28 | 29 | 56 |

The number of transitions between the current levels 0, 1 and 2 was used to compute on the basis of Eq. (1) the number of channels present in the multi-channel recording shown in Fig. 6, while confirming the validity of the binomial distribution in this case.

ment provided strong support for three independent channels characterized by identical open probability. In fact, a throughout analysis of two other experimental records with, respectively, three and four current levels led to the conclusion that the multi-channel activity observed in these experiments was representative of an homogeneous channel population constituted of ionic pores with identical conducting and gating properties.

The overall voltage dependence of the channel open probability, $P_o$, in 200 mmol/l (cis)/50 mmol/l (trans) $CaCl_2$ conditions is presented in Fig. 7. Data were collected from four different experiments where stationarity could be confirmed for potential values ranging from −55 mV to 80 mV. The channel showed a weak voltage dependence with $P_o$ increasing slightly at negative potentials. On the basis of the results presented in Table 2, this increase in open probability at negative potentials could be related to a decrease at negative potentials of the channel mean closed time ($1/T_{0\to1}$) coupled to an increase of the channel mean open time ($1/T_{1\to0}$). The channel mean open time and mean closed time at positive potential were estimated at 20 ± 10 ms, and 100 ± 20 ms, respectively. This particular channel is not expected therefore to be affected in a significant manner by physiologically relevant changes in membrane potential.

### 3.3. Action of blocking agents

Fig. 8 shows examples of single channel recordings carried out in 200 mmol/l (cis)/50 mmol/l (trans) $CaCl_2$ conditions where the effect of the $Cl^-$ channel blockers, NPPB, DPC and DIDS was investi-

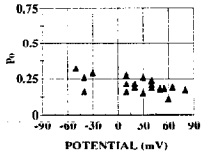


Fig. 7. Effect of voltage on the channel open probability measured in 200 mmol/l (cis)/50 mmol/l (trans) $CaCl_2$ conditions. Results are from four different experiments. The channel showed a weak voltage dependence over the voltage range considered (−60 mV to 70 mV), with an increase in open probability at hyperpolarizing potentials (0.18 at 65 mV compared to 0.33 at −55 mV).

gated. The current traces illustrated in Fig. 8A and C provide clear indications that NPPB at 100 μM and DIDS at 300 μM can significantly inhibit channel activity whereas DPC at concentrations up to 500 μM failed to cause an important channel block (Fig. 8B). No effect of NPPB was observed, however, at concentrations ranging from 1 to 10 μM. In contrast, an important inhibition was induced following the

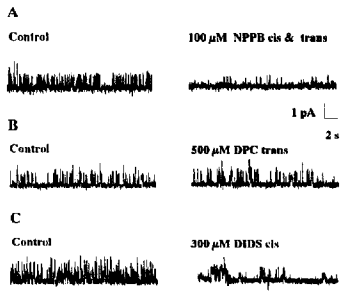


Fig. 8. Effect of $Cl^-$ channel blockers on channel activity. Single channel recordings performed in 200 mmol/l (cis)/50 mmol/l (trans) $CaCl_2$ conditions. The applied voltage was equal to 30 mV. (A) The addition in trans and cis chamber of 100 μM NPPB caused a near complete inhibition of channel activity. (B) Slight inhibitory effect caused by DPC at high concentration (500 μM) on channel activity. (C) Effect of 300 μM DIDS added to the cis chamber. Signal filtered at 100 Hz and digitized at 500 Hz.

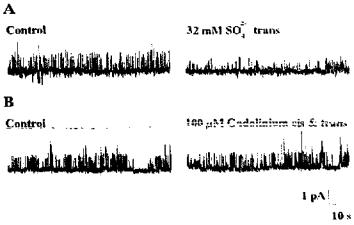


Fig. 9. Ion block of the 14 pS channel. Single channel recordings performed in 200 mmol/l (cis)/50 mmol/l (trans) $CaCl_2$ conditions. The applied voltage was equal to -40 mV. (A) Inhibitory effect observed with 32 mM $(NH_4)_2SO_4$ in the cis solution. (B) The addition on both sides of the membrane of 100 μM $Gd^{3+}$ failed to inhibit channel activity. Signal filtered at 100 Hz and digitized at 500 Hz.

addition of $SO_4^{2-}$ (32 mmol/l) to the trans compartment (Fig. 9A). The presence of $SO_4^{2-}$ caused in this case a 30 ± 9-fold ($n = 3$) decrease in mean current value, due mainly to a variation of the channel open probability. Finally, the effect of the trivalent cation $Gd^{3+}$, a blocker of non-selective ionic channels in several cell types was tested [20]. The results obtained indicate that the addition of $Gd^{3+}$ at a supra maximal concentration of 100 μM on either side of the membrane failed to cause a significant decrease in single channel activity ($n = 5$).

### 3.4. Effect of phosphorylation

The transcellular transport of $Cl^-$ ions in renal cells has been reported to be strongly regulated by hormones linked to the adenylate cyclase pathway [1,14]. Fig. 10A presents an example of single channel recording in which the effect of the catalytic subunit of protein kinase A (PKA) was tested following incorporation of the 14 pS channel. No significant effect of PKA was detected at concentrations less than 20 U/ml ($n = 3$). In the example illustrated in Fig. 10A, the normalized mean current value $NP_o$ taken over 2 min was found to increase from 0.17 pA to 0.45 pA following addition into the trans chamber of 60 U/ml of catalytic subunit of PKA. A detailed analysis revealed that the observed increase was due to both a change in $P_o$ from 0.08 to 0.15 coupled to a variation in the number of channels from 2 to 3. The increase in $P_o$ was essentially related to a decrease in the channel mean closed time (300 ms to 120 ms) with no significant change in the channel mean open time (20 ms). A similar behaviour was observed in two additional experiments carried out at concentration of PKA catalytic subunit ranging from 60 U/ml to 80 U/ml. The mean number of open channels ($NP_o$) increased on the average 2.7-fold and this effect was related to a variation of both $P_o$ and $N$. The observed variation in the number of active channels may have been caused either by the activation of silent channels that were already incorporated into

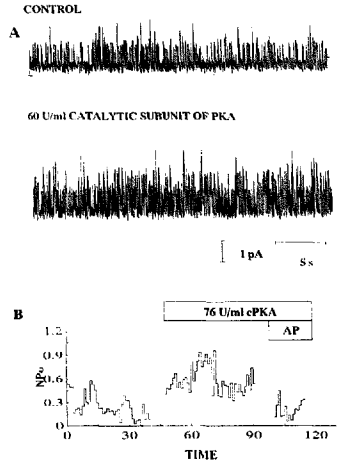


Fig. 10. Activation by the catalytic subunit of protein kinase A (cPKA). Single channel recordings performed in 200 mmol/l $CaCl_2$ (cis)/50 mmol/l NMDG-Cl (trans) conditions. The applied voltage was equal to 40 mV throughout. The trans solution contained 2 mmol/l ATP and 2 mmol/l $Mg^{2+}$. Stimulation of channel activity following the trans addition of 60 U/ml of the catalytic subunit of PKA. (B) Effect of the catalytic subunit of PKA (76 U/ml) on the mean number of open channels, $NP_o$, followed by the inhibitory action of 60 U/ml alkaline phosphatase (AP) added to the trans solution. Values of $NP_o$ were computed by averaging the current over successive 1 s periods. Signal filtered at 130 Hz and digitized at 1500 Hz.

the bilayer or by the incorporation of new channels. This latter effect may be consequent to the fusion of vesicles onto the membrane in response to an increased ionic permeability. These two possibilities can not currently be discriminated on the basis of these recordings alone. An example of the observed changes in $NP_o$ following the addition into the trans chamber solution of the catalytic subunit of PKA is presented in Fig. 10B. This example also indicates that the stimulating effect of PKA can be reversed with a non specific protein phosphatase, such as alkaline phosphatase (AP), added into the trans solution (60 U/ml). These results strongly suggest that the gating of this 14 pS channel is controlled to some extent via a cAMP-dependent phosphorylation process. The observed PKA-induced channel activation appeared rather specific, since the addition of the catalytic subunit of PKA failed to affect the activity of a $Cl^-$ channel of large conductance that was present in two of the experiments where an activation of the 14 pS was observed.

## 4. Discussion

This study presents the first characterization of an ionic channel obtained by fusion onto a lipid bilayer of vesicles prepared from native apical membranes of isolated rabbit distal tubules. The present work provided evidence for an anionic channel of 14 pS with a relative permeability to $Na^+$ over $Cl^-$ ion, $P_{Na}/P_{Cl} < 0.1$. The channel reconstitution approach was chosen to avoid the potential problems related to the various degrees of cell dedifferentiation which takes place during cell culturing. Several lines of evidence suggest that the vesicles used for the experiments described in this work are representative of the apical membrane of the distal tubule. For instance, these vesicles were shown not to be enriched in alkaline phosphatase (proximal tubule) or Na-K-ATPase (basolateral membrane), but to possess a $Na^+$ transport sensitive to thiazides [15,16]. Up to now, only luminal membranes coming from rabbit connecting tubules and from the principal cells of the cortical collecting duct present this characteristic [21]. It has to be mentioned that due to the absence of specific membrane markers for the apical membrane of the distal tubule, the exact orientation of these vesicles remains still poorly defined. We can not therefore rule out the possibility that some channels were incorporated such that their cytosolic domain was in contact with the cis solution. However, the results of the binomial analysis shown in Fig. 6 seem to indicate that the observed 14 pS channels constituted an homogeneous channel population with the same conductance and identical gating properties. In addition, we can not currently rule out the possibility that the vesicle preparation used for our experiments contained vesicles formed from contaminant membranes with better fusion properties. The likelihood that the observed single channel activity arose from contaminant membranes is remote, however, given that the fusion of the vesicles with the bilayer was induced mechanically and was therefore less dependent on the intrinsic fusion properties of the vesicle preparations.

### 4.1. Channel characterization

Cyclic AMP-activated $Cl^-$-selective channels with slope conductance within the 9 pS to 12 pS range have already been identified at the apical membrane of several renal cell preparations [5,10,22]. For instance, Poncet et al. [10] have shown the presence at the apical membrane of rabbit distal bright convoluted tubule cells (DCTb) in primary culture, of a $Cl^-$ channel of small conductance (9 pS) activated by cAMP. This channel appeared voltage-insensitive and could not be blocked by cytosolic applications of 10 $\mu$M NPPB or DPC. A near complete inhibition was observed, however, at high DPC concentrations (1 mmol/l). Similarly, a $Cl^-$-selective channel of 9 pS has been identified by Ling et al. [5] in the apical membrane of rabbit cortical collecting duct cells (CCT) grown in primary culture. The incidence and open probability of this channel were found to increase by treating the cells with forskolin or with permeable analogues of cAMP. This channel, in addition, exhibited a linear current/voltage relationship and appeared unaffected by DIDS. Finally, a voltage-independent $Cl^-$ channel of 8 pS was reported by Marunaka and Eaton [22] in distal nephron A6 cells. These results are in agreement with the present finding of a distal tubule $Cl^-$ channel of small conductance (11 pS in NaCl conditions) with weakly voltage-dependent gating properties. In addition, as for the channels observed in DCTb cells, the

single channel recordings presented in Figs. 3, 5 and 8 provide evidence for a relatively low sensitivity to blocking agents such as NPPB and DPC. However, our results indicate an inhibitory effect of DIDS at concentrations ranging from 150 $\mu$M (data not shown) to 300 $\mu$M (Fig. 9C). This is at variance with the observations reported on CCT and DCTb cells, where $Cl^-$ channel activity remained unchanged after DIDS application. Pharmacological properties similar to the ones illustrated in Fig. 9 have also been reported for a cAMP activated $Cl^-$ channel of small conductance identified in the basolateral membrane of the mouse thick ascending limb [7]. Not only could this channel be totally blocked by NPPB and DPC at 100 $\mu$M and 1 mmol/l, respectively, but DIDS was also effective at inhibiting channel activity at a sub-millimolar concentration. Finally, the demonstration of an inhibitory effect by DIDS and the fact that ATP was not essential for channel activity strongly suggest that, despite some functional similarities with CFTR, the 14 pS identified belongs to a different $Cl^-$ channel family [23,24].

Inhibition was also observed using divalent anions. The results in Fig. 9A show for instance a total inhibition of channel activity following the addition of 32 mmol/l $SO_4^{2-}$ in the trans compartment. $SO_4^{2-}$ has been reported to block a number of $Cl^-$-selective channels via a single-site competitive blocking process (see for instance [25]). Half inhibition was usually observed at concentrations ranging from 10 to 50 mmol/l and appeared to be function of the $Cl^-$ ion concentration. A total inhibitory effect at 32 mmol/l is thus fully compatible with values reported for the $SO_4^{2-}$ binding affinity. In contrast, there was a lack of inhibitory effect by $Gd^{3+}$. This would argues against the possibility that the 14 pS channel measured by incorporation may be related to the stretch activated non-selective channels identified in several distal and proximal tubule cell preparations [26–28].

### 4.2. Channel phosphorylation

The results in Fig. 10A and B show the effect of the catalytic subunit of PKA (60 U/ml to 80 U/ml) on the 14 pS channel activity. Both the number of active channels, $N$, and the channel open probability, $P_o$, were found to be affected. This conclusion is supported by single channel analysis performed using the Baum–Welch re-estimation algorithm which also revealed that the observed changes in open probability caused by PKA resulted from a decrease in the channel mean closed time, with no significant variations in the channel mean open time. This would suggest that part of the action of PKA consists in promoting channel openings rather than stabilizing one or several of the channel conducting states. Interestingly, the effect of the catalytic subunit of PKA could be cancelled by adding a non specific protein phosphatase such as alkaline phosphatase (Fig. 10B). These experiments confirmed therefore that the activity of the 14 pS channel can be controlled to some extent via an increase in cAMP. Our observations contrast, however, with the findings reported from cell attached experiments carried on DCTb and CCT cells, where an increase in intracellular cAMP had no effect on the activity of spontaneously active $Cl^-$ channels [10], but rather increased the number of active channels without significant changes in channel open probability. Similar observations have been reported for the intestinal and tracheal $Cl^-$ channels, namely, that PKA activates quiescent channels while having no effect on the activity of already active channels [29]. Our results do not rule out the possibility that PKA activates channels that were incorporated but silent. However, an increase in the number of active channels in our case is always interpretable in terms of fusion of additional vesicles onto the lipid bilayer. In addition, the patch clamp results on DCTb cells have indicated a loss of channel activity within seconds following membrane excision. This observation is difficult to reconciliate with the present results where channel activity was recorded and maintained following incorporation into a black lipid membrane. Spontaneous $Cl^-$ channel activity could be nevertheless recorded following patch excision from the basolateral membrane of the mouse thick ascending limb [7]. In this case, channel activity increased during exposure to ATP. No similar effect of ATP (1 mmol/l) was observed on the 14 pS channel obtained by incorporation.

### 4.3. Physiological role

One must be careful in extrapolating results from channel incorporation experiments to the in vivo situation. There will always be some uncertainties

concerning the exact origin of the channel obtained by incorporation. As a result, discussions on the role of reconstituted channels remain limited. Theoretically, activation of a channel with an ion selectivity profile like the one described in the present work should lead to a depolarization of the cell potential to approximately −30 mV. Accordingly, if $Na^+$ and/or $Ca^{2+}$ reabsorption is stimulated, the resulting apical membrane depolarization would cause $Cl^-$ reabsorption, maintaining a favourable electrochemical gradient for $Na^+$ and/or $Ca^{2+}$ entry. Conversely, apical membrane hyperpolarization would promote $Cl^-$ secretion, as long as the $Cl^-$ ion activity remains elevated above electrochemical equilibrium. Experiments carried out on the principal cells of rabbit cortical collecting ducts and on cultured cells from the mouse distal tubule have confirmed that the intracellular $Cl^-$ activity is above the electrochemical equilibrium in these cases [8,30], favouring the hypothesis of a $Cl^-$ secretion in response to a cell hyperpolarization.

## 5. Conclusions

We have identified, using vesicles prepared from apical membranes of rabbit distal tubules, a $Cl^-$ permeable channel of small conductance with pharmacological properties distinct from those of the CFTR channel family. Because channel activity could be enhanced in the presence of the catalytic subunit of PKA, it is suggested that the observed channel may contribute to changes in $Cl^-$ ion permeability at the apical membrane of the distal tubule in response to hormone stimulation.

## Acknowledgements

This work was supported by a grant from the Kidney Foundation of Canada.

## References

[1] Simmons, N.L. (1993) Exp. Physiol. 78, 117–137.
[2] Chalfant, M.L., Coupaye-Gerard, B. and Kleyman, T.R. (1993) Am. J. Physiol. 264, C1480–C1488.
[3] Marunaka, Y. and Tohda, H. (1993) Biochim. Biophys. Acta 1153, 105–110.
[4] Poncet, V., Tauc, M., Bidet, M. and Poujeoul, P. (1994) Am. J. Physiol. 266, F543–F553.
[5] Ling, B.N., Kokko, K.E. and Eaton, D.C. (1994) J. Clin. Invest. 93, 829–837.
[6] Dietl, P. and Stanton, B.A. (1992) Am. J. Physiol. 263, F243–F250.
[7] Guinamard, R., Chraïbi, A. and Teulon, J. (1995) J. Physiol. (London) 485, 92–112.
[8] Gesek, F.A. and Friedman, P.A. (1992) J. Clin. Invest. 90, 749–758.
[9] Friedman, P.A. and Gesek F.A. (1993) Am. J. Physiol. 264, F181–F198.
[10] Poncet, V., Merot, J. and Poujeol, P. (1992) Pflügers Arch. 422, 112–119.
[11] Chraïbi, A., Van den Abbeele, T., Guinamard, R. and Teulon, J. (1994) Pflügers Arch. 429, 90–97.
[12] Matsunaga, H., Stanton, B.A., Gesek, F.A. and Friedman, P.A. (1994) Am. J. Physiol. 267, C157–C165.
[13] Merot, J., Poncet, V., Bidet, M., Tauc, M. and Poujeol, P. (1991) Biochim. Biophys. Acta 1070, 387–400.
[14] Reeves, W.B., Winters, C.J., Zimniak, L. and Andreoli, T.E. (1994) Adv. Nephrol. 23, 177–190.
[15] Bouhtiauy, I., Lajeunesse, D. and Brunette, M.G. (1991) Endocrinology 128, 251–258.
[16] Brunette, M.G., Mailloux, J. and Lajeunesse, D. (1992) Kidney Int. 41, 281–288.
[17] Chung, S.H., Moore, J.B., Xia, L.G., Premkumar, L.S. and Gage, P.W. (1990) Phil. Trans. R. Soc. Lond. B. 329, 265–285.
[18] Morier, N. and Sauvé, R. (1994) Biophys. J. 67, 590–602.
[19] Kendall, M. and Stuart, A.G. (1961) The advanced theory of statistics, Vol. 2, Charles Griffin, London and High Wycombe.
[20] Yang, X.C. and Sachs, F. (1989) Science 243, 1068–1071.
[21] Ellison, D.H., Velazquez, H. and Wright, F.S. (1987) Am. J. Physiol. 253, F546–F554.
[22] Marunaka, Y. and Eaton, D.C. (1990) Am. J. Physiol. 258, C352–C368.
[23] Anderson, M.P., Sheppard, D.N., Berger, H.A. and Welsh, M.J. (1992) Am. J. Physiol. 263, L1–L4.
[24] Welsh, M.J., Anderson, M.P., Rich, D.P., Berger, H.A., Denning, G.M., Ostedgaard, L.S., Sheppard, D.N., Cheng, S.H., Gregory, R.J. and Smith, A.E. (1992) Neuron 8, 821–829.
[25] Tanifuji, M., Sokabe, M. and Kasai, M. (1987) J. Membr. Biol. 99, 103–111.
[26] Hurst, A.M. and Hunter, M. (1990) J. Physiol. (London) 430, 13–24.
[27] Robson, L. and Hunter, M. (1994) Pflügers Arch. 429, 98–106.
[28] Ubl, J., Murer, H. and Kolb, H.A. (1988) J. Membr. Biol. 104, 223–232.
[29] Winters, C.J., Reeves, W.B. and Andreoli, T.E. (1992) J. Membr. Biol. 128, 27–39.
[30] Sauer, M., Dorge, A., Thuraw, K. and Beck, F.X. (1989) Pflügers Arch. 413, 651–655.